New Journal of Physics

The open access journal at the forefront of physics

CrossMark

PAPER

Quantum dynamics of propagating photons with strong interactions: a generalized input–output formalism

Tommaso Caneva[1,3], Marco T Manzoni[1,3], Tao Shi[2,3], James S Douglas[1], J Ignacio Cirac[2] and Darrick E Chang[1]

1   ICFO-Institut de Ciencies Fotoniques, The Barcelona Institute of Science and Technology, 08860 Castelldefels (Barcelona), Spain
2   Max-Planck-Institut für Quantenoptik, Hans Kopfermann-strasse 1, D-85748 Garching, Germany
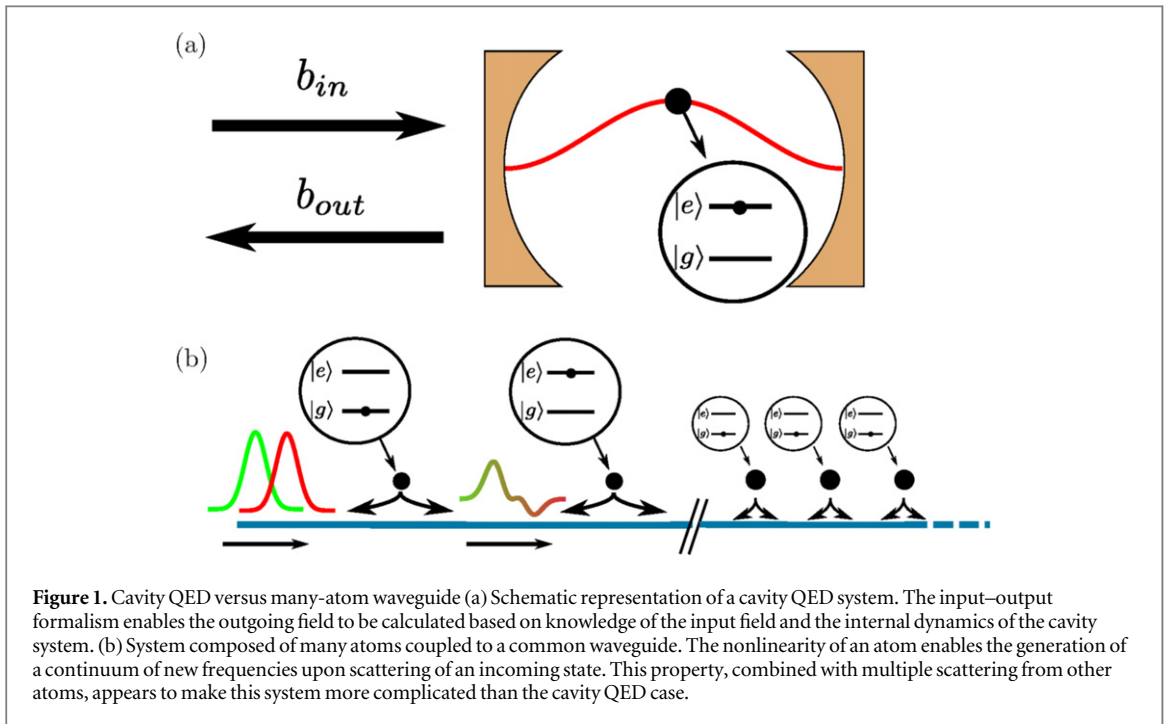3   These authors contributed equally to the work

E-mail: darrick.chang@icfo.es

Abstract

There has been rapid development of systems that yield strong interactions between freely propagating photons in one-dimension via controlled coupling to quantum emitters. This raises interesting possibilities such as quantum information processing with photons or quantum many-body states of light, but treating such systems generally remains a difficult task theoretically. Here, we describe a novel technique in which the dynamics and correlations of a few photons can be exactly calculated, based upon knowledge of the initial photonic state and the solution of the reduced effective dynamics of the quantum emitters alone. We show that this generalized 'input–output' formalism allows for a straightforward numerical implementation regardless of system details, such as emitter positions, external driving, and level structure. As a specific example, we apply our technique to show how atomic systems with infinite-range interactions and under conditions of electromagnetically induced transparency enable the selective transmission of correlated multi-photon states.

1. Introduction

Systems in which individual photons can interact strongly with each other constitute an exciting frontier for the fields of quantum and nonlinear optics [1]. Such systems enable the generation and manipulation of non-classical light, which are crucial ingredients for quantum information processing and quantum networks [2]. At the many-body level, it has been predicted that these systems can produce phenomena such as quantum phase transitions of light [3–5] or photon crystallization [6, 7]. Early examples of such systems where strong interactions between photons could be observed consisted of individual atoms coupled to single modes of high-finesse optical cavities, within the context of cavity quantum electrodynamics (QEDs) [8, 9]. More recently, a number of systems have emerged that produce strong optical nonlinearities between freely propagating photons, including cold atomic gases coupled to guided modes of tapered fibers [10, 11], photonic crystal fibers [12] or waveguides [13], cold Rydberg gases in free space [14], and superconducting qubits coupled to microwave waveguides [15, 16].

The paradigm of cavity QED admits exact analytical or numerical solutions at the few-photon (and/or few-atom) level through the elegant 'input–output' formalism [17], as illustrated conceptually in figure 1(a). In this formalism, all of the properties of the field exiting the system (the output) can be determined based upon knowledge of the input field and the dynamics of the atom-cavity system alone. For a few excitations, the latter can be solved due to the small Hilbert space associated with a small number of excitations of a discrete cavity mode. In contrast, despite rapid development on the experimental front, theoretical techniques to treat the dynamics of freely propagating photons interacting with spatially distributed emitters are generally lacking. At first glance, the challenge compared to the cavity case arises from the fact that a two-level system is a nonlinear frequency mixer, which is capable of generating a continuum of new frequencies from an initial pulse, as schematically depicted in figure 1(b). *A priori*, keeping track of this continuum as it propagates and re-scatters

Figure 1. Cavity QED versus many-atom waveguide (a) Schematic representation of a cavity QED system. The input–output formalism enables the outgoing field to be calculated based on knowledge of the input field and the internal dynamics of the cavity system. (b) System composed of many atoms coupled to a common waveguide. The nonlinearity of an atom enables the generation of a continuum of new frequencies upon scattering of an incoming state. This property, combined with multiple scattering from other atoms, appears to make this system more complicated than the cavity QED case.

from other emitters appears to be a difficult task. An exception is the weak excitation limit, in which atoms can be treated as linear scatterers and the powerful transfer matrix method of linear optics can be employed [18, 19].

The full quantum case has been solved exactly in a limited number of situations in which nonlinear systems are coupled to 1D waveguides [20–30]. The formalism employed in [21] is particularly elegant, because it establishes an input–output relation to determine the nonlinear scattering from a two-level atom. Here, we show that this technique can be efficiently generalized to many atoms, chiral or bi-directional waveguides, and arbitrary atomic configurations, providing a powerful tool to investigate nonlinear optical dynamics in all systems of interest.

This paper is organized in the following way: first, we present a generalized input–output formalism to treat few-photon propagation in waveguides coupled to many atoms. We show that the infinite degrees of freedom associated with the photonic modes can be effectively integrated out, yielding an open, interacting 'spin' model that involves only the internal degrees of freedom of the atoms. This open system can be solved using a number of conventional, quantum optical techniques. Then, we show that the solution of the spin problem can be used to re-construct the optical fields. In particular, we provide a prescription to map spin correlations to S-matrix elements, which contain full information about the photon dynamics, and give explicit closed-form expressions for the one- and two-photon cases. Importantly, in analogy with the cavity QED case, our technique enables analytical solutions under some scenarios, but in general allows for simple numerical implementation under a wide variety of circumstances of interest, such as different level structures, external driving, atomic positions, atomic motion, etc. Finally, to illustrate the ease of usage, we apply our technique to the study of nonlinear field propagation through an optically dense ensemble of atoms with Rydberg-like interactions.

2. Generalized input–output formalism

In this section we consider a generic system composed of many atoms located at positions z_i along a bidirectional waveguide. We assume that there is an optical transition between ground and excited-state levels $|g\rangle$ and $|e\rangle$ to which the waveguide couples, but otherwise we leave unspecified the atomic internal structure and the possible interactions between them (e.g., Rydberg interactions), as such terms do not affect the derivation presented here. The bare Hamiltonian of the system is composed of a term describing the energy levels of the atoms H_{at}, and a waveguide part $H_{ph} = \sum_{\nu=\pm} \int dk \, \omega_k b_{\nu,k}^\dagger b_{\nu,k}$, where k is the wavevector and $\nu = \pm$ is an index for the direction of propagation, with the plus (minus) denoting propagation towards the right (left) direction. We assume that within the bandwidth of modes to which the atoms significantly couple, the dispersion relation for the guided modes can be linearized as $\omega_k = c|k|$. The interaction between atoms and photons is given in the rotating wave approximation by

$$H_{\text{int}} = g \sum_{v=\pm} \sum_{i=1}^{N} \int \mathrm{d}k \left(b_{v,k} \sigma_{eg}^{i} \, \mathrm{e}^{\mathrm{i}vkz_i} + \text{h.c.} \right), \tag{1}$$

which describes the process where excited atoms can emit photons into the waveguide, or ground-state atoms can become excited by absorbing a photon. The coupling amplitude g is assumed to be identical for all atoms, while the coupling phase depends on the atomic position ($\mathrm{e}^{\mathrm{i}vkz_i}$). Here, we will explicitly treat the more complicated bidirectional case, although all of the results readily generalize to the case of a single direction of propagation.

Our immediate goal is to generalize the well-known input–output formalism of cavity QED [17] and the more recent formalism for a single atom coupled to a waveguide [21], to the present situation of many spatially distributed atoms coupled to a common waveguide. In short, we will eliminate the photonic degrees of freedom by formal integration, which reveals that the output field exiting the collection of atoms is completely describable in terms of the input field and atomic properties alone. This formal integration also provides a set of generalized Heisenberg–Langevin equations that governs the atomic evolution.

The Heisenberg equations of motion for σ_{ge}^{i} and $b_{v,k}$ can be readily obtained by calculating the commutators with H. To simplify the presentation of the resulting equations, we replace the spin operators σ_{ge}^{i} with the bosonic annihilation operator a_i. The two-level nature of the atomic transition can be retained by introducing an interaction energy U_0 for multiple excitations, through the term $(U_0/2)\sum_i a_i^{\dagger} a_i (a_i^{\dagger} a_i - 1)$ in H_{at}, and by taking the limit $U_0 \to \infty$ at the end of calculations for observable quantities.

The Heisenberg equations for $b_{v,k}$ can be formally integrated and Fourier transformed, to obtain the real-space wave equation

$$b_v(z, t) = b_{v,\text{in}}(t - vz/c) - \frac{\mathrm{i}\sqrt{2\pi} g}{c} \sum_{j=1}^{N} \theta\left(v\left(z - z_j \right) \right) a_j\left(t - \frac{v\left(z - z_j \right)}{c} \right). \tag{2}$$

Here $b_{v,\text{in}}$ is the homogeneous solution, physically corresponding to the freely propagating field in the waveguide, while the second term on the right consists of the part of the field emitted by the atoms. Inserting equation (2) into the equation for a_i, we obtain

$$\dot{a}_i = \mathrm{i}\left[H_{\text{at}}, a_i \right] - \mathrm{i}\sqrt{2\pi} g \sum_{v=\pm} b_{v,\text{in}}\left(t - vz_i/c \right) - \frac{2\pi g^2}{c} \sum_{j=1}^{N} a_j\left(t - \left| z_i - z_j \right|/c \right). \tag{3}$$

In realistic systems, time retardation can be neglected, resulting in the Markov approximation $a_j(t - |z_i - z_j|/c) \approx a_j(t) \mathrm{e}^{\mathrm{i}\omega_{\text{in}}|z_i - z_j|/c}$. Here, ω_{in} is a central frequency around which the atomic dynamics is centered (typically the atomic resonance frequency). This approximation is valid when the difference in free-space propagation phases $\Delta\omega L/c \ll 1$ is small across the characteristic system size L and over the bandwidth of photons $\Delta\omega$ involved in the dynamics. As a simple example, the characteristic bandwidth of an atomic system is given by its spontaneous emission rate, corresponding to a few MHz, which results in a significant free-space phase difference only over lengths $L \gtrsim 1$ m much longer than realistic atomic ensembles. A more general theory which does not require the Markov approximation is presented in [31].

We have thus obtained the generalized Heisenberg–Langevin equation

$$\dot{a}_i = \mathrm{i}\left[H_{\text{at}}, a_i \right] - \mathrm{i}\sqrt{\frac{c\,\Gamma_{\text{1D}}}{2}} \sum_{v=\pm} b_{v,\text{in}}\left(t - vz_i/c \right) - \frac{\Gamma_{\text{1D}}}{2} \sum_{j=1}^{N} a_j \, \mathrm{e}^{\mathrm{i}\omega_{\text{in}}|z_i - z_j|/c}, \tag{4}$$

where we have identified $\Gamma_{\text{1D}} = 4\pi g^2/c$ as the single-atom spontaneous emission rate into the waveguide modes. If we keep separated the terms proportional to a_j coming from the right and left-going photonic fields, we can find easily that the Lindblad jump operators corresponding to the decay of the atoms into the waveguide are $O_{\pm} = \sqrt{\Gamma_{\text{1D}}/4} \sum_j a_j \mathrm{e}^{\mp \mathrm{i}\omega_{\text{in}}z_j/c}$, in terms of which we can write the master equation for the atomic density matrix $\dot{\rho} = \mathcal{L}[\rho] \equiv -\mathrm{i}[H_{\text{at}}, \rho] + \sum_{v=\pm} 2O_v \rho O_v^{\dagger} - O_v^{\dagger} O_v \rho - \rho O_v^{\dagger} O_v$. We also see that we can derive equation (4) from a non-Hermitian effective Hamiltonian

$$H_{\text{eff}} = H_{\text{at}} - \frac{\mathrm{i}\Gamma_{\text{1D}}}{2} \sum_{ij} a_i^{\dagger} a_j \, \mathrm{e}^{\mathrm{i}\omega_{\text{in}}|z_i - z_j|/c}, \tag{5}$$

which can be used for a quantum jump description of the atomic dynamics. The resulting infinite-range interaction between a pair of atoms i, j intuitively results from the propagation of a mediating photon between that pair, with a phase factor proportional to the separation distance.

Within the same approximations employed above to derive the Heisenberg–Langevin equations we can obtain a generalized input–output relation of the form $b_{v,\text{out}}(z, t) = b_{v,\text{in}}(t - vz/c) - \mathrm{i}\sqrt{\Gamma_{\text{1D}}/(2c)} \sum_{i=1}^{N} a_i(t) \mathrm{e}^{\mathrm{i}v\omega_{\text{in}}(z - z_i)/c}$, where the output field is defined for $z > z_R \equiv \max[z_i]$ ($z < z_L \equiv \min[z_i]$) for right(left)-going fields. However, since the right-going output field propagates freely after z_R, it is convenient to simply define $b_{+,\text{out}}(t) = b_{+,\text{out}}(z_R + \epsilon, t)$ as the field immediately past the right-most atom (where ϵ is an

infinitesimal positive number), and similarly for the left-going output. The derived relation shows that the outgoing field properties are obtainable from those of the atoms alone.

The emergence of infinite-range interactions between emitters mediated by guided photons, and input–output relationships between these emitters and the outgoing field, have been discussed before in a number of contexts [19, 21, 32], but the idea that such concepts could be used to study quantum interactions of photons in extended systems has not been fully appreciated. In the remaining sections, we will demonstrate the effectiveness of this approach to quantum nonlinear optics. In particular, the infinite-dimensional continuum of the photons is effectively reduced to a Hilbert space of dimension $\dim[\mathcal{H}] = \sum_{i=0}^{n} \binom{n}{k}$ where n is the maximum number of atomic excitations (for $n = N$ we have $\dim[\mathcal{H}] = 2^N$). The atomic dynamics, on the other hand, having been reduced to standard Heisenberg–Langevin equations, quantum jump, or master equations, are solvable by conventional prescriptions [33]. It is also possible to derive generalized master equations describing the atomic dynamics in response to arbitrary (e.g., non-classical) incident states of light, as detailed in appendix C.

3. Relation to S-matrix elements

The S-matrix characterizes how an incoming state of monochromatic photons evolves via interaction with atoms into a superposition of outgoing monochromatic photons. Because monochromatic photons form a complete basis, the S-matrix thus contains all information about photon dynamics. Here, we will show that S-matrix elements can be calculated from the dynamics of the atoms evolving under the effective spin model.

Formally, the S-matrix for the interaction of an n-photon state with an arbitrary system is defined as

$$
\begin{aligned}
S_{\mathbf{p};\mathbf{k}}^{(n)} &= \langle \mathbf{p}|\, S\, |\mathbf{k}\rangle \\
&= \langle 0|\, b_{\text{out}}(p_1) .. b_{\text{out}}(p_n) b_{\text{in}}^\dagger(k_1) .. b_{\text{in}}^\dagger(k_n)|0\rangle \\
&= FT^{(2n)} \langle 0|\, b_{\text{out}}(t_1) .. b_{\text{out}}(t_n) b_{\text{in}}^\dagger(t'_1) .. b_{\text{in}}^\dagger(t'_n)|0\rangle,
\end{aligned}
\tag{6}
$$

where the input and output creation operators respectively create freely propagating incoming and outgoing photonic states. The vectors $\mathbf{p}$ and $\mathbf{k}$ denote the outgoing and incoming frequencies of the n photons. The input and output operators can be any combination of $+$ and $-$ propagation directions (we have omitted this index here for simplicity). In the last line we have used a global Fourier transformation $FT^{(2n)} = (2\pi)^{-n} \int \prod_{i=1}^{n} \, \mathrm{d}t_i \mathrm{d}t'_i \, \mathrm{e}^{\mathrm{i}c(t_i p_i - t'_i k_i)}$, to express the S-matrix in time.

The S-matrix has been calculated exactly before in a limited number of situations [20, 21, 27, 30]. Here, we provide a general prescription to numerically obtain the S-matrix starting from the input–output formalism. One can also find a similar set of conclusions that was derived simultaneously and independently in [34]. First, it should be noted that the operators b_{in} and b_{out} correspond to the input and output operators defined in the previous section [21]. On the other hand, the input–output relation enables the correlator of equation (6) to be written purely in terms of atomic operators. For notational simplicity, we give a derivation for a single spin and a monodirectional waveguide, but its generalization to the bidirectional waveguide and many atoms is straightforward. For our purpose it is enough to have an input–output relation of the form
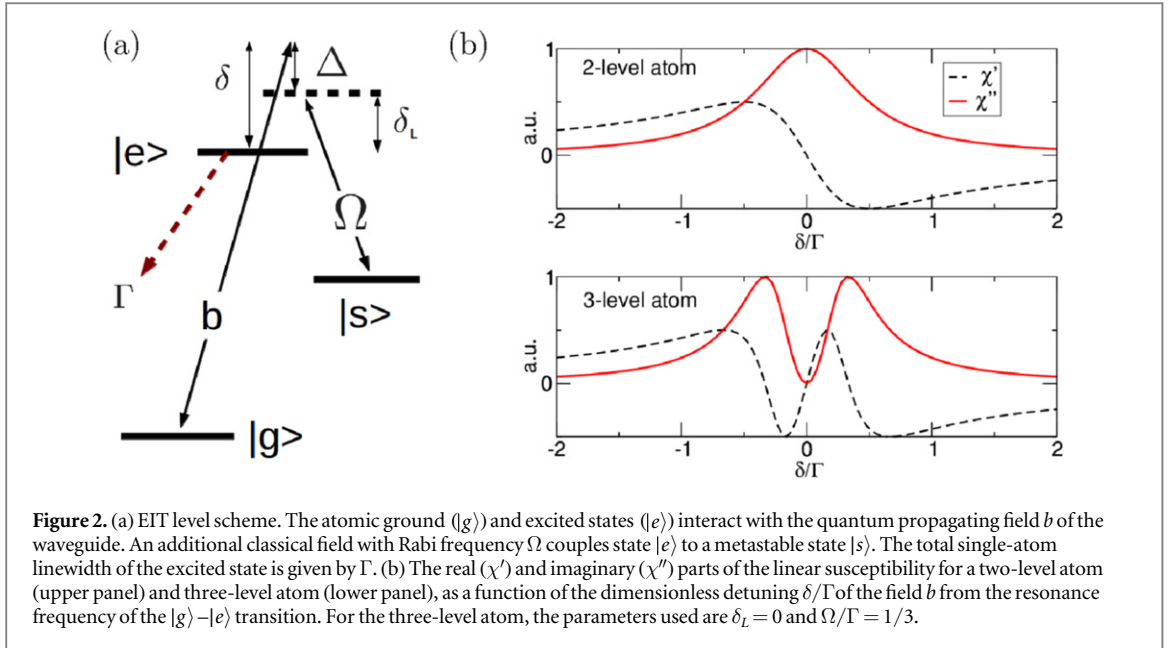
$$
b_{\text{out}} = b_{\text{in}} - \mathrm{i}\sqrt{\gamma} a,
\tag{7}
$$

where a is in our case the spin operator σ_{ge}.

We summarize the main idea of the derivation here, while the details can be found in appendix A.1. We begin by noting that equation (7) enables one to replace output operators by a combination of system and input operators, or input operators by system and output operators. Selectively using these substitutions, one can exploit favorable properties of either the input or output field, in order to gradually time order all of the system operators (where operators at later times appear to the left of those at earlier times), while removing input and output operators from the correlation. The favorable properties that can be used are that (1) system and input operators commute $[a(t), b_{\text{in}}(t')] = 0$, when $t' > t$, and likewise $[a(t), b_{\text{out}}(t')] = 0$ for $t' < t$, (2) input annihilation operators at different times commute amongst themselves, as do output annihilation operators, and (3) the correlator can be reduced in size using $[b_{\text{in}}(t), b_{\text{in}}^\dagger(t')] = \delta(t - t')$, or made to vanish using $b_{\text{in}}(t)|0\rangle = 0$ or $\langle 0| b_{\text{out}}^\dagger(t) = 0$. Through this procedure, the S-matrix can be expressed as a Fourier transform of a sum of terms involving only time-ordered atomic operators (indicated by the operator T). These functions generally have the form

$$
\langle 0|\, T\big[a(t_1) .. a(t_m) a^\dagger(t'_1) .. a^\dagger(t'_m)\big]|0\rangle,
\tag{8}
$$

with $m \leqslant n$, multiplied by $n-m$ delta functions in time.

Figure 2. (a) EIT level scheme. The atomic ground ($|g\rangle$) and excited states ($|e\rangle$) interact with the quantum propagating field b of the waveguide. An additional classical field with Rabi frequency Ω couples state $|e\rangle$ to a metastable state $|s\rangle$. The total single-atom linewidth of the excited state is given by Γ. (b) The real (χ') and imaginary (χ'') parts of the linear susceptibility for a two-level atom (upper panel) and three-level atom (lower panel), as a function of the dimensionless detuning δ/Γ of the field b from the resonance frequency of the $|g\rangle-|e\rangle$ transition. For the three-level atom, the parameters used are $\delta_L = 0$ and $\Omega/\Gamma = 1/3$.

Moreover, using the general expression for the Heisenberg–Langevin equation and the quantum regression theorem, it can be proven that when external fields driving the system do not generate waveguide photons, the correlation function of equation (8) can be evaluated by evolving $a(t)$ as $\mathrm{e}^{iH_{\mathrm{eff}}t}\, a\, \mathrm{e}^{-iH_{\mathrm{eff}}t}$ (see appendix A.2 for a formal derivation). Here, H_{eff} is the effective Hamiltonian from equation (5) that contains only the spin operators. Although such a form for $a(t)$ is not true in general due to quantum noise, these noise terms have no influence on the correlation. A similar procedure as above enables one to express other important observables of the field, such as the second-order correlation function $g^{(2)}(t)$, in terms of correlation functions involving atoms alone.

While the discussion has thus far been completely general, the case of S-matrix elements involving only one or two photons can be formally reduced to particularly simple expressions. For example, in appendix B, we show that the transmission coefficient T_k for the many-atom, bi-directional waveguide case is related to the S-matrix by $S^{(1)}_{p+;k+} \equiv \langle 0|\, b_{+,\mathrm{out}}(p)b^{\dagger}_{+,\mathrm{in}}(k)|0\rangle \equiv T_k \delta_{pk}$. Furthermore, it can be expressed in terms of a known $\sim N \times N$ matrix corresponding to the single-excitation Green's function G_0 (whose form varies depending on the system details)

$$T_k = 1 - \frac{i\Gamma_{1D}}{2}\sum_{ij}\Big[G_0(k)\Big]_{ij}\mathrm{e}^{-ik_{\mathrm{in}}(z_i-z_j)}. \tag{9}$$

Similarly, the two-photon S-matrix in transmission is generally given by

$$\begin{aligned}S^{(2)}_{p_1+,p_2+;k_1+,k_2+} &= T_{k_1}T_{k_2}\delta_{p_1k_1}\delta_{p_2k_2}\\ &\quad -i\frac{\Gamma_{1D}^2}{8\pi}\delta_{p_1+p_2,k_1+k_2}\sum_{iji'j'}W_{ij}T_{ij;i'j'}W_{i'j'} + \big(p_1 \leftrightarrow p_2\big),\end{aligned} \tag{10}$$

where the first and second terms on the right describe the linear and nonlinear contributions, respectively. The latter term can be expressed in terms of matrices W related to the single-excitation Green's function, and a known $\sim N^2 \times N^2$ matrix T characterizing atomic nonlinearities and interactions.

4. Electromagnetically induced transparency

In this section, we apply our formalism to a specific example involving three-level atoms under conditions of electromagnetically induced transparency (EIT) and with Rydberg-like interactions between atoms [14]. The linear susceptibility for a two-level atom with states $|g\rangle$ and $|e\rangle$, in response to a weak probe field with detuning $\delta = \omega_p - \omega_{eg}$ from the atomic resonance, is shown in figure 2(b). It can be seen that the response on resonance is primarily absorptive, as characterized by the imaginary part of the susceptibility (χ'', red curve). In contrast, the response can become primarily dispersive near resonance if a third level $|s\rangle$ is added, and if the transition $|e\rangle - |s\rangle$ is driven by a control field (characterized by Rabi frequency Ω and single photon detuning $\delta_L = \omega_L - \omega_{es}$). Specifically, via interference between the probe and control fields, the medium can become

transparent to the probe field ($\chi'' = 0$) when two-photon resonance is achieved, $\delta - \delta_L = 0$, realizing EIT [35]. In this process, the incoming probe field strongly mixes with spin wave excitations σ_{sg} to create 'dark-state polaritons'. The medium remains highly transparent within a characteristic bandwidth Δ_{EIT} around the two-photon resonance, which reduces to $\Delta_{EIT} \sim 2\Omega^2/(\Gamma\sqrt{D})$, when $\delta_L = 0$. Here we have introduced the total single-atom linewidth Γ (see below) and the optical depth D, corresponding to the opacity of the medium in the absence of EIT and defined in terms of input and output intensity as $I_{out}(\Omega = 0)/I_{in}(\Omega = 0) = \exp(-D)$. These dark-state polaritons propagate at a strongly reduced group velocity $v_g \ll c$, which is proportional to the control field intensity [35], as indicated by the steep slope of the real part of the susceptibility χ' in figure 2(b).

Taking s_i to be the annihilation operator for the state $|s_i\rangle$, EIT is described within our spin model by the effective spin Hamiltonian

$$H = -\left(\delta_L + i\frac{\Gamma'}{2}\right)\sum_j a_j^\dagger a_j - \Omega\sum_j \left(a_j^\dagger s_j + s_j^\dagger a_j\right) - i\frac{\Gamma_{1D}}{2}\sum_{j,l} e^{ik_{in}|z_j - z_l|}a_j^\dagger a_l, \qquad (11)$$

where the first two terms represents the explicit form of H_{at} in equation (5) for the EIT three-level atomic structure. In addition to the waveguide coupling, here we have added an independent atomic decay rate Γ' into other channels (e.g., unguided modes), yielding a total single-atom linewidth of $\Gamma = \Gamma' + \Gamma_{1D}$.

Our theoretical model nearly ideally describes experiments in which atoms are coupled to one-dimensional waveguides such as nanofibers [10] or photonic crystals [11], in which the interaction probability of a single photon and atom $\Gamma_{1D}/\Gamma \sim 0.1$ can be significant and up to $N \sim 10^3$ atoms are trapped. One consequence of the large interaction probability is that even a single atom can yield a significant reflectance for single photons [11]. In free-space experiments, the atom–photon interaction probability is much smaller, while a much larger number of atoms is used to induce a significant optical response. While this large number cannot be implemented numerically with our model, our system can nonetheless be used to reproduce macroscopic observables, thus making our approach an excellent description for atom-light interfaces in general.
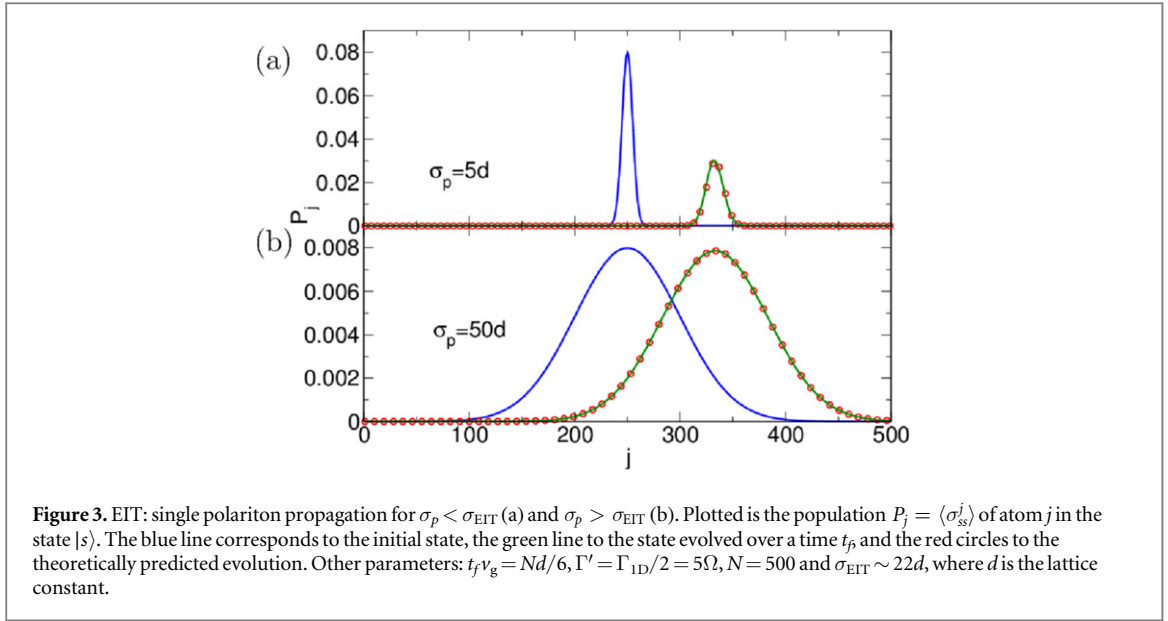
Intuitively (and as can be rigorously shown, see below), provided that free-space experiments only involve a single transverse mode of light, one expects that the system response to light only depends on the interaction probability and number of atoms via their product. This product in fact defines the optical depth[4] $D = 2N\Gamma_{1D}/\Gamma$. As $D \lesssim 10^2$ in free-space experiments, such systems can be evaluated using our spin model with several hundred atoms and suitably large Γ_{1D}/Γ. The only remaining issue is the potentially large reflection generated by atoms in the mathematical model, compared to free-space ensembles where reflection is negligible. Reflection can be suppressed in the model by giving the atoms a lattice constant d where $k_{in}d = (2m + 1)\pi/2$, where m is a non-negative integer, such that the reflection from atoms destructively interferes[5] [36]. All subsequent numerical calculations are performed under this condition.

The spin model on a lattice describing EIT, equation (11), can be exactly solved in the linear regime using the transfer matrix formalism [36], which correctly reproduces the free-space result and dependence on optical depth for the group velocity $v_g = 2\Omega^2/(n\Gamma_{1D})$ and transparency window Δ_{EIT}, where n is the (linear) atomic density. The corresponding minimum spatial extent of a pulse that can propagate inside the medium with high transparency is given by $\sigma_{EIT} = v_g/\Delta_{EIT}$.

A single photon propagating inside an ensemble of atoms under EIT conditions is coherently mapped onto a single dark polariton, corresponding to a delocalized spin wave populating the single excitation subspace of the atomic ensemble. The polariton dynamics can be therefore visualized directly by monitoring the excitation probability $\langle \sigma_{ss}^j \rangle$ of the atoms in the ensemble. In figure 3, we initialize a single polariton inside the medium with an atomic wave function of the form $|\psi\rangle = \sum_j f_j \sigma_{sg}^j |g\rangle^{\otimes N}$, and we determine numerically the time evolution under H in equation (11) up to a final time t_f. Choosing an initially Gaussian spin wave, $f_j = \exp(ik_{in}dj)\exp(-(jd - \mu)^2/4\sigma_p^2)/(2\pi\sigma_p^2)^{1/4}$, with spatial extent σ_p (blue line), one sees that the wavepacket propagates a distance $v_g \cdot t_f$, and with little loss provided that $\sigma_p > \sigma_{EIT}$. Numerics (green line) show perfect agreement with theoretical predictions (red circles) obtained via the transfer matrix formalism [36].

---

[4] Actually the formula $D = 2N\Gamma_{1D}/\Gamma$ is derived in the limit $\Gamma' \gg \Gamma_{1D}$, where for a two-level atom the transmission on resonance is given by $t = 1 - (\Gamma_{1D}/\Gamma) \simeq \exp(-\Gamma_{1D}/\Gamma)$. Such a regime of high transmission per single atom is relevant for the majority of EIT experiments and indeed, as shown in the main text, known results of EIT are reproduced correctly. However in the opposite limit $\Gamma' \ll \Gamma_{1D}$ a single atom behaves like a perfect mirror [42] ($t \simeq 0$) and the correct theoretical description requires a different expansion for the transmission coefficient, $t = 1 - (\Gamma_{1D}/\Gamma) \simeq \Gamma'/\Gamma_{1D}$.

[5] In the complementary case where $k_{in}d = m\pi$, reflections from atoms constructively interfere and atomic mirrors can be realized as shown in [19].

Figure 3. EIT: single polariton propagation for $\sigma_p < \sigma_{EIT}$ (a) and $\sigma_p > \sigma_{EIT}$ (b). Plotted is the population $P_j = \langle \sigma_{ss}^j \rangle$ of atom j in the state $|s\rangle$. The blue line corresponds to the initial state, the green line to the state evolved over a time t_f, and the red circles to the theoretically predicted evolution. Other parameters: $t_f v_g = Nd/6$, $\Gamma' = \Gamma_{1D}/2 = 5\Omega$, $N = 500$ and $\sigma_{EIT} \sim 22d$, where d is the lattice constant.

5. Infinite range interaction

The spin model formalism can be easily extended to include arbitrary atomic interactions, providing a powerful tool to study quantum nonlinear optical effects. As a concrete example, we consider a system in which atoms can interact directly over a long range, such as via Rydberg states [7, 37, 38] or photonic crystal bandgaps [39, 40]. The total Hamiltonian is given by

$$H = -\left(\delta_L + i\frac{\Gamma'}{2}\right)\sum_j a_j^\dagger a_j - \Omega \sum_j \left(a_j^\dagger s_j + s_j^\dagger a_j\right)$$
$$- i\frac{\Gamma_{1D}}{2}\sum_{j,l} e^{ik_{in}|z_j - z_l|} a_j^\dagger a_l + \frac{1}{2}\sum_{j\neq l} U_{jl} s_j^\dagger s_l^\dagger s_l s_j$$
$$+ H_{drive} \tag{12}$$

in which U_{jl} represents a dispersive interaction between atoms j and l when they are simultaneously in state $|s\rangle$. As we are primarily interested in demonstrating the use of our technique, we take here a 'toy model' where atoms experience a constant infinite-range interaction, $U_{jl} \equiv C$. Such a case enables the numerical results to be intuitively understood, although we note that other choices of U_{jl} do not increase the numerical complexity. In particular we are interested in studying the propagation of a constant weak coherent input field through the atomic ensemble. The corresponding driving then is given by $H_{drive} = \sqrt{\frac{c\Gamma_{1D}}{2}} \mathcal{E} \sum_j (a_j^\dagger e^{ik_{in}z_j} e^{-i\Delta t} + a_j e^{-ik_{in}z_j} e^{i\Delta t})$, where $\sqrt{\frac{c\Gamma_{1D}}{2}} \mathcal{E} \ll \Gamma$ is the amplitude of the constant driving field, $\Delta = \delta - \delta_L$ the detuning from two photon resonance condition, and the initial state is given by the global atomic ground state $|\psi_i\rangle = |g\rangle^{\otimes N}$ [41, 42]. With infinite-range interaction, one spin flip to state $|s\rangle_{\bar{j}}$ shifts the energies of all other states $|s\rangle_j$ by an amount $C/2$. A second photon should then be able to propagate with perfect transparency, provided it has a detuning compensating for the energy shift $C/2$, thus ensuring the two-photon resonance condition is satisfied. As a result, we expect to see a transparency window for two photons, whose central frequency shifts linearly with $C/2$.

This predicted behavior can be confirmed by plotting the transmitted intensity fraction, $T_1 = I/I_{in} = \langle b_{+,out}^\dagger(t) b_{+,out}(t)\rangle/\mathcal{E}^2$, and also the second-order correlation function $T_2 = \langle b_{+,out}^\dagger(t) b_{+,out}^\dagger(t) b_{+,out}(t) b_{+,out}(t)\rangle/\mathcal{E}^4$, which corresponds roughly to the two-photon transmission. Figures 4(a), (b) shows the single-photon transmission T_1 and two-photon transmission T_2 as a function of the interaction strength C and detuning from two photon resonance Δ. As expected, T_1 shows a peak at $\Delta = 0$ independently of the interaction intensity C; instead the peak in T_2 shifts towards $\Delta = C/2$ with increasing C. The decay of T_2 for increasing C can be intuitively understood by noting that we have a constant coherent state input, in which photons are randomly spaced, causing two photons to enter the medium at different times. Thus, until the second photon enters, the first photon propagates as a single polariton detuned by Δ from the single-photon transparency condition, getting partially absorbed in the process. By increasing the interaction we increase the detuning for this single polariton and consequently its absorption, explaining the trend observed for T_2 in figure 4(b). A quantitative description of this phenomenon is given in appendix D.
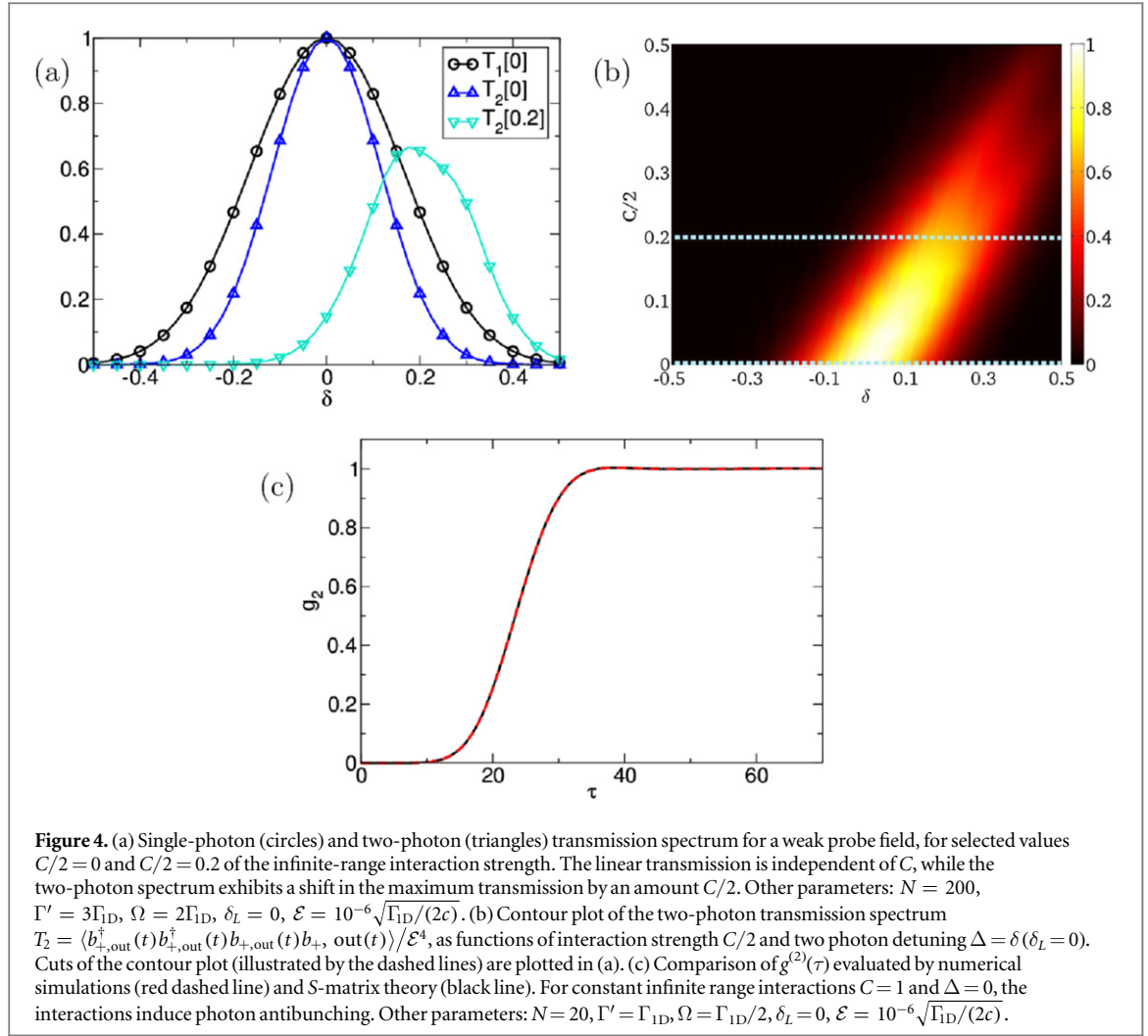
Figure 4. (a) Single-photon (circles) and two-photon (triangles) transmission spectrum for a weak probe field, for selected values $C/2 = 0$ and $C/2 = 0.2$ of the infinite-range interaction strength. The linear transmission is independent of C, while the two-photon spectrum exhibits a shift in the maximum transmission by an amount $C/2$. Other parameters: $N = 200$, $\Gamma' = 3\Gamma_{1D}$, $\Omega = 2\Gamma_{1D}$, $\delta_L = 0$, $\mathcal{E} = 10^{-6}\sqrt{\Gamma_{1D}/(2c)}$. (b) Contour plot of the two-photon transmission spectrum $T_2 = \langle b^\dagger_{+,\text{out}}(t) b^\dagger_{+,\text{out}}(t) b_{+,\text{out}}(t) b_{+,\text{out}}(t)\rangle / \mathcal{E}^4$, as functions of interaction strength $C/2$ and two photon detuning $\Delta = \delta$ ($\delta_L = 0$). Cuts of the contour plot (illustrated by the dashed lines) are plotted in (a). (c) Comparison of $g^{(2)}(\tau)$ evaluated by numerical simulations (red dashed line) and S-matrix theory (black line). For constant infinite range interactions $C = 1$ and $\Delta = 0$, the interactions induce photon antibunching. Other parameters: $N = 20$, $\Gamma' = \Gamma_{1D}$, $\Omega = \Gamma_{1D}/2$, $\delta_L = 0$, $\mathcal{E} = 10^{-6}\sqrt{\Gamma_{1D}/(2c)}$.

Field correlation functions like intensity $I = \langle b^\dagger_{+,\text{out}}(t) b_{+,\text{out}}(t)\rangle$ or $g_2(\tau) = \langle b^\dagger_{+,\text{out}}(t) b^\dagger_{+,\text{out}}(t + \tau) b_{+,\text{out}}(t + \tau) b_{+,\text{out}}(t)\rangle / I^2$ can be computed according to the following strategy. First we switch from Heisenberg representation to Schrödinger representation, so that for the intensity we get: $I = \langle b^\dagger_{+,\text{out}}(t) b_{+,\text{out}}(t)\rangle = \langle\psi(t)|b^\dagger_{+,\text{out}} b_{+,\text{out}}|\psi(t)\rangle$. The time evolved wave function, $|\psi(t)\rangle$, is determined by numerically evolving the initial spin state $|\psi_i\rangle$ under H for a time t. Then, the state immediately after detection of one photon, $b_{+,\text{out}}|\psi(t)\rangle = |\phi\rangle$, is evaluated by expressing $b_{+,\text{out}}$ in terms of spin operators using the input–output formalism: $b_{+,\text{out}} = \mathcal{E}e^{ik_{\text{in}}z_R} - i\sqrt{\Gamma_{1D}/(2c)} \sum_j a_j e^{ik_{\text{in}}(z_R - z_j)}$. Finally we obtain the intensity by computing the probability of the one-photon detected state, $I = \langle\phi|\phi\rangle$.

For $g_2(\tau)$ an extra step is needed. Its numerator describes the process of detecting two photons, the first at time t and the second at time $t + \tau$: $f(t + \tau) = \langle b^\dagger_{+,\text{out}}(t) b^\dagger_{+,\text{out}}(t + \tau) b_{+,\text{out}}(t + \tau) b_{+,\text{out}}(t)\rangle$. As before we can switch to the Schrödinger picture, $f(t + \tau) = \langle\psi(t)|b^\dagger_{+,\text{out}} e^{iH\tau} b^\dagger_{+,\text{out}} b_{+,\text{out}} e^{-iH\tau} b_{+,\text{out}}|\psi(t)\rangle$, and evaluate the state after detection of the first photon, $b_{+,\text{out}}|\psi(t)\rangle = |\phi\rangle$. Then detection of a second photon after a time τ entails performing an extra evolution under H and annihilating a photon, that is: $b_{+,\text{out}} e^{-iH\tau}|\phi\rangle = b_{+,\text{out}}|\phi(\tau)\rangle$. Finally, we evaluate the quantity $f(t + \tau) = \langle\phi(\tau)|b^\dagger_{+,\text{out}} b_{+,\text{out}}|\phi(\tau)\rangle$, by again expressing $b_{+,\text{out}}$ in terms of spin operators. In figure 4(c), we plot the numerically obtained result for $g^{(2)}(\tau)$, for the case where infinite-range interactions are turned on ($C = 1$) and for a weak coherent input state with detuning $\Delta = 0$. In such a situation, one expects for the single-photon component of the coherent state to transmit perfectly, while the two-photon component is detuned from its transparency window and becomes absorbed. This nonlinear absorption intuitively yields the strong anti-bunching dip $g^{(2)}(\tau) = 0 < 1$. We also evaluate this second-order correlation function using the analytical result for the two-photon S-matrix in equation (10), which shows perfect agreement as expected.

6. Conclusion

We have shown that the dynamics of a few photons, propagating under strong interactions mediated by quantum emitters, is fully and efficiently characterized by the dynamics of an open quantum spin model. As the

spin model is solvable by standard quantum optical techniques for open systems, our approach provides an easily implementable recipe for the exact numerical study of a large class of quantum nonlinear optical systems. As an example, it provides an attractive alternative to numerical simulations of propagation through cold Rydberg gases, where typically the continuous field is finely discretized and its degrees of freedom are explicitly kept track of [37]. Our technique can also be used to treat a number of strongly nonlinear systems based upon atomic saturation [6], where only approximate effective theories for field propagation were previously available. Furthermore, it would be interesting to explore connections wth conceptually related systems, such as quantum emitters coupled to waveguides beyond the rotating wave aproximation [43], and chiral [44] or other spin chains [45]. We anticipate that the availability of exact results will greatly aid in the development of effective theories for the generally challenging problem of quantum many-body states of light, and that our model will shed new insight on conceptual links between such systems and quantum spin systems.

Acknowledgments

Appendix A. Scattering theory

A.1. Connecting *S*-matrix to atomic correlation functions

We present here the full derivation of the decomposition of the *S*-matrix elements in terms of time-ordered atomic correlation functions. The starting point is the definition of the *S*-matrix in equation (6). Since the output operators commute between themselves because of the indistinguishability of photons, they can be freely ordered by decreasing times. Introducing the time ordering operator T and also using equation (7), the operators in equation (6) can be written as

$$T\left[\left(b_{in}\left(t_1\right) + \sqrt{\gamma}a\left(t_1\right)\right)..\left(b_{in}\left(t_n\right) + \sqrt{\gamma}a\left(t_n\right)\right)\right]b_{in}^\dagger\left(t'_1\right)..b_{in}^\dagger\left(t'_n\right). \tag{A.1}$$

It is natural to label the terms above by the number m of system operators a present in each term. Thanks to the fact that $[a(t), b_{in}(t')] = 0$ for $t' > t$, all the input operators can be moved to the right of the spin operators. Thus, the term of order m will be of the form

$$\langle 0|\ T\left[a\left(t_1\right)..a\left(t_m\right)\right]b_{in}\left(t_{m+1}\right)..b_{in}\left(t_n\right)b_{in}^\dagger\left(t'_1\right)..b_{in}^\dagger\left(t'_n\right)|0\rangle, \tag{A.2}$$

and can be simplified using the commutation relations between input operators $[b_{in}(t), b_{in}^\dagger(t')] = \delta(t - t')$. This manipulation results in a sum of $(n!)^2/(m!)^2(n - m)!$ terms for each original term of order m. Each term of the sum consists of $n - m$ delta functions multiplied by a correlation function of the form

$$\langle 0|\ T\left[a\left(t_1\right)..a\left(t_m\right)\right]b_{in}^\dagger\left(t'_1\right)..b_{in}^\dagger\left(t'_m\right)|0\rangle. \tag{A.3}$$

Since the a operators commute with the $b_{in}^\dagger$ operators at later times, the time ordering operator can be extended to all the operators in the correlation function. Using again equation (7) to express the input operators one gets

$$\langle 0|\ T\left[a\left(t_1\right)..a\left(t_m\right)\left(b_{out}^\dagger\left(t'_1\right) - \sqrt{\gamma}a^\dagger\left(t'_1\right)\right)..\left(b_{out}^\dagger\left(t'_m\right) - \sqrt{\gamma}a^\dagger\left(t'_m\right)\right)\right]|0\rangle. \tag{A.4}$$

However, since the operators $b_{out}^\dagger$ commute with all the operators a on the left, only

$$\langle 0|\ T\left[a\left(t_1\right)..a\left(t_m\right)a^\dagger\left(t'_1\right)..a^\dagger\left(t'_m\right)\right]|0\rangle \tag{A.5}$$

remains, which reproduces equation (8).

A.2. Evolution under the effective Hamiltonian

In equation (8) the vacuum state $|0\rangle$ stands for $|0\rangle_b |g\rangle^{\otimes N}$, i.e., the vacuum state of field modes and the ground state of all the atoms. The atomic operators are in the Heisenberg picture, $a(t) = e^{iHt}ae^{-iHt}$, and H is the Hamiltonian of the whole system without the driving field. By taking the term with $t_1 > t_2 > ... > t_m > t'_1 > t'_2 > ... > t'_m$ as an example (our argument holds for any time ordering), we show now that equation (8) can be evaluated by effectively evolving system operators as $a(t) = e^{iH_{eff}t}ae^{-iH_{eff}t}$. The quantum regression theorem is applied here to eliminate the bath or photonic degree of freedom, and results in

$$\langle 0|_b \langle g|^{\otimes N} a\left(t_1\right)... a\left(t_m\right)a^\dagger\left(t'_1\right)... a^\dagger\left(t'_m\right)|0\rangle_b |g\rangle^{\otimes N} = Tr\left[ae^{\mathcal{L}\left(t_1-t_2\right)}a ... a^\dagger e^{\mathcal{L}\left(t_{m-1}-t_m\right)}a^\dagger \rho(0)\right], \quad\quad (A.6)$$

where $\rho(0) = |g\rangle^{\otimes N} \langle g|^{\otimes N} |0\rangle_b \langle 0|$ and $\mathcal{L}$ is the Lindblad super-operator of the system, defined in the main text. $\mathcal{L}$ contains a deterministic part, which generates an evolution driven by H_{eff} and which conserves the number of excitations, and a jump part, which reduces the number of atomic excitations. Because of the form of the correlators, which contain an equal number of atomic creation and annihilation operators, the jump part of the evolution of the operators gives a vanishing contribution to the correlation function, proving what was stated above.

Appendix B. Examples of *S*-matrix elements

In this section of the appendix we provide explicit examples of how to use the results derived above to calculate specific matrix elements. In particular we present the case of the scattering of (1) *n* photons on a two-level atom coupled to a one-directional waveguide and (2) one and two photons scattering on a Rydberg-EIT system.

B.1. *n* photons scattering on a single two-level atom

The *S*-matrix element $S^{(n)}$ for the scattering of *n* photons can be in general decomposed in a part that is a series of products of lower-order elements and a part that cannot be expressed in such a way. The latter is called the fully connected part of the matrix element and physically corresponds to a *n*-body interaction, and is denoted by $i\mathcal{T}^{(n)}$. Thus, knowing how to decompose the *S*-matrix, one has to calculate $i\mathcal{T}^{(j)}$ with $1 \leqslant j \leqslant n$ to construct $S^{(n)}$. Furthermore, it can be shown that the fully connected part in an element of order *n* can be obtained by the system correlation function of order *n*. We show here how to calculate such elements using the results presented above, for the case of a single two-level atom coupled to a one-directional waveguide. It will be possible to appreciate the simplicity of our formalism compared the more cumbersome method used in [30] to obtain the same result.

We start from the relation between the connected part of the matrix element and the correlation function of atomic operators

$$i\mathcal{T}^{(n)}_{[\mathbf{p};\mathbf{k}]} = \frac{(-\Gamma)^n}{(2\pi)^n}\int\prod_{i=1}^{n} dt_i \, dt'_i \, e^{i\left(p_i t_i - k_i t'_i\right)}\left\langle T\tilde{\sigma}_-\left(t_n\right)... \tilde{\sigma}_-\left(t_1\right)\tilde{\sigma}_+\left(t'_n\right)... \tilde{\sigma}_+\left(t'_1\right)\right\rangle, \quad\quad (B.1)$$

where $\tilde{\sigma}_-(t) = e^{iH_{\text{eff}}t}\sigma_- e^{-iH_{\text{eff}}t}$, with $H_{\text{eff}} = (\omega_{eg} - i\Gamma/2)\sigma_{ee}$. The time ordering in the correlator gives $(2n)!$ possible orderings, but it is easy to arrive to the conclusion that only orderings which start on the left with a σ_- operator and alternate σ_+ and σ_- give a non-zero contribution. It is also immediate to see that the number of this possible orderings is $(n!)^2$. A possible ordering is for instance

$$\left\langle \tilde{\sigma}_-\left(t_n\right)\tilde{\sigma}_+\left(t'_n\right) .. \tilde{\sigma}_-\left(t_1\right)\tilde{\sigma}_+\left(t'_1\right)\right\rangle, \quad\quad (B.2)$$

which, expressing explicitly the time dependence, is equal to

$$\left\langle \sigma_- e^{-iH_{\text{eff}}\left(t_n-t'_n\right)}\sigma_+ .. \sigma_- e^{-iH_{\text{eff}}\left(t_1-t'_1\right)}\sigma_+\right\rangle. \qu\quad (B.3)$$

Since H_{eff} is diagonal in the $|g\rangle$, $|e\rangle$ basis, we can insert identity operators between the σ operators in the form of $|g\rangle\langle g| + |e\rangle\langle e|$ in order to evaluate the Hamiltonians in the exponents. We immediately end up with $\prod_{i=1}^{n} e^{-i\alpha(t_i-t'_i)}$ where we have defined $\alpha = \omega_{eg} - i\Gamma/2$. Inserting this result in equation (B.1) we get

$$i\mathcal{T}^{(n)}_{[\mathbf{p};\mathbf{k}]} = \frac{(-\Gamma)^n}{(2\pi)^n}\int_{-\infty}^{+\infty} dt_n \int_{-\infty}^{t_n} dt'_n ... \int_{-\infty}^{t_1} dt'_1\left[\prod_{i=1}^{n} e^{i\left(p_i-\alpha\right)t_i} \, e^{-i\left(k_i-\alpha\right)t'_i} + \text{perms.}\right], \qu\quad (B.4)$$

where the permutations are over the two sets of incoming and outgoing photon frequencies k_i and p_i. The integral gives

$$i\mathcal{T}^{n}_{[\mathbf{p};\mathbf{k}]} = - 2\pi i\left(\frac{\Gamma}{2\pi}\right)^n\left\{\prod_{l=1}^{n-1}\left(\sum_{i=1}^{l}\Delta_i\right)^{-1} \prod_{m=1}^{n}\left(k_m - \alpha + \sum_{i=1}^{m-1}\Delta_i\right)^{-1} + \text{perms.}\right\}$$

$$\times\, \delta\left(\sum_{i=1}^{n}\Delta_i\right), \qu\quad (B.5)$$

where $\Delta_i = k_i - p_i$, which coincides with the result of [30].

B.2. One and two-photon scattering on a Rydberg-EIT system

The effective Hamiltonian of the Rydberg-EIT system is given by

$$H_{\text{eff}} = H_0 + H_{\text{HC}} + \frac{1}{2}\sum_{ij} U_{ij} s_i^\dagger s_j^\dagger s_j s_i, \tag{B.6}$$

where H_0 is given by equation (11), and the hardcore interaction is

$$H_{\text{HC}} = \frac{U_0}{2}\sum_j \left(a_j^\dagger a_j + s_j^\dagger s_j\right)\left(a_j^\dagger a_j + s_j^\dagger s_j - 1\right) \tag{B.7}$$

with $U_0 \to \infty$ corresponding to the three-level atom.

For the single incident right moving photon with momentum k, it follows from equations (6) and (8) that the S-matrix element is

$$S_{p+;k+}^{(1)} = \delta_{pk} - \int_{-\infty}^{+\infty} \frac{\mathrm{d}t\,\mathrm{d}t'}{\pi} e^{\mathrm{i}\left(pt-kt'\right)}\langle 0|\ \mathcal{T}\tilde{O}_+(t)\tilde{O}_+^\dagger(t')|0\rangle, \tag{B.8}$$

with

$$O_+ = \sqrt{\frac{\Gamma_{\text{1D}}}{4}}\sum_j a_j e^{-\mathrm{i}k_{\text{in}}z_j}. \tag{B.9}$$

This element describes the amplitude of a single transmitted photon with momentum p, using the time ordered correlation function of the system operator. We set for notational simplicity the speed of light $c = 1$. The second term of $S_{p+;k+}^{(1)}$, i.e., the Fourier transform of the correlator

$$\int_{-\infty}^{+\infty} \frac{\mathrm{d}t\,\mathrm{d}t'}{\pi} e^{\mathrm{i}\left(pt-kt'\right)}\langle 0|\ \mathcal{T}\tilde{O}_+(t)\tilde{O}_+^\dagger(t')|0\rangle = \frac{\mathrm{i}\Gamma_{\text{1D}}}{4\pi}\delta_{pk}\sum_{ij} e^{-\mathrm{i}\left(k_{\text{in}}+k\right)\left(z_i-z_j\right)}\left[G_0(k)\right]_{ij}^{aa} \tag{B.10}$$

can be obtained from the Green's function $G_0(\omega) = 1/(\omega - \mathcal{H}_1)$ with the single-particle Hamiltonian

$$\mathcal{H}_1 = \begin{pmatrix} \left(-\delta_L - \mathrm{i}\dfrac{\Gamma'}{2}\right)\delta_{ij} - \mathrm{i}\dfrac{\Gamma_{\text{1D}}}{2}e^{\mathrm{i}k_{\text{in}}|z_i-z_j|} & \Omega\delta_{ij} \\ \Omega\delta_{ij} & 0 \end{pmatrix}. \tag{B.11}$$

Here, we have expressed $\mathcal{H}_1$ in the basis $\{|a_i\rangle,\ |s_i\rangle\}$, and $[G_0(k)]_{ij}^{\sigma\sigma'}$ denotes the element $\langle\sigma_i|\ G_0(k)\left|\sigma_j'\right\rangle$ with $\sigma,\ \sigma' = a, s$. The element $S_{p+;k+}^{(1)} \equiv T_k\delta_{pk}$ gives rise to the transmission coefficient

$$T_k = 1 - \mathrm{i}\frac{\Gamma_{\text{1D}}}{2}\sum_{ij}\left[G_0(k)\right]_{ij}^{aa}e^{-\mathrm{i}k_{\text{in}}\left(z_i-z_j\right)}. \tag{B.12}$$

For two right-going incident photons with momenta k_1 and k_2, the two-photon S-matrix element $S_{p_1+,p_2+;k_1+,k_2+}^{(2)}$ describes the amplitude to a final state with two transmitted photons of momenta p_1 and p_2. By equations (6) and (8) in the main text, we find that

$$S_{p_1+,p_2+;k_1+,k_2+}^{(2)} = T_{k_1}T_{k_2}\left(\delta_{p_1k_1}\delta_{p_2k_2} + \delta_{p_1k_2}\delta_{p_2k_1}\right)$$
$$+ \frac{\Gamma_{\text{1D}}^2}{4(2\pi)^2}\sum_{i_1i_2}\sum_{j_1j_2} e^{-\mathrm{i}k_{\text{in}}\left(z_{i_1}+z_{i_2}\right)}G_{i_1i_2;j_1j_2}^{aa;aa}\left(p_1,\ p_2;\ k_1,\ k_2\right)e^{\mathrm{i}k_{\text{in}}\left(z_{j_1}+z_{j_2}\right)}, \tag{B.13}$$

with

$$G_{i_1i_2;j_1j_2}^{aa;aa}\left(p_1,\ p_2;\ k_1,\ k_2\right)$$
$$= \int \mathrm{d}t_1'\,\mathrm{d}t_2'\,\mathrm{d}t_1\,\mathrm{d}t_2\, e^{\mathrm{i}\left(p_1t_1'+p_2t_2'-k_1t_1-k_2t_2\right)}\left\langle \mathcal{T}\tilde{a}_{i_1}\left(t_1'\right)\tilde{a}_{i_2}\left(t_2'\right)\tilde{a}_{j_1}^\dagger\left(t_1\right)\tilde{a}_{j_2}^\dagger\left(t_2\right)\right\rangle_c \tag{B.14}$$

Here, $\left\langle \mathcal{T}\tilde{a}_{i_1}(t_1')\tilde{a}_{i_2}(t_2')\tilde{a}_{j_1}^\dagger(t_1)\tilde{a}_{j_2}^\dagger(t_2)\right\rangle_c$ denotes the connected four-point Green's function, which involves an interaction between the two excitations in the system. The S-matrix also contains terms arising from disconnected correlation functions, e.g., $\left\langle \mathcal{T}\tilde{a}_{i_1}(t_1')\tilde{a}_{j_1}^\dagger(t_1)\right\rangle\left\langle \mathcal{T}\tilde{a}_{i_2}(t_2')\tilde{a}_{j_2}^\dagger(t_2)\right\rangle$ describing the linear propagation of each excitation separately, which yields the term in (B.14) proportional to $T_{k_1}T_{k_2}$.

The interaction between two excitations under the Hamiltonian $H_{\text{HC}} + \sum_{ij}U_{ij}s_i^\dagger s_j^\dagger s_j s_i/2$ can be represented by the ladder diagram shown in figure B1. This diagram is represented mathematically by the two-body T-matrix, $T(E)$, which satisfies the Lippmann–Schrödinger equation

$$\mathbf{T}(E) = \mathbf{U} + \mathbf{U}\Pi_0(E)\mathbf{T}(E). \tag{B.15}$$
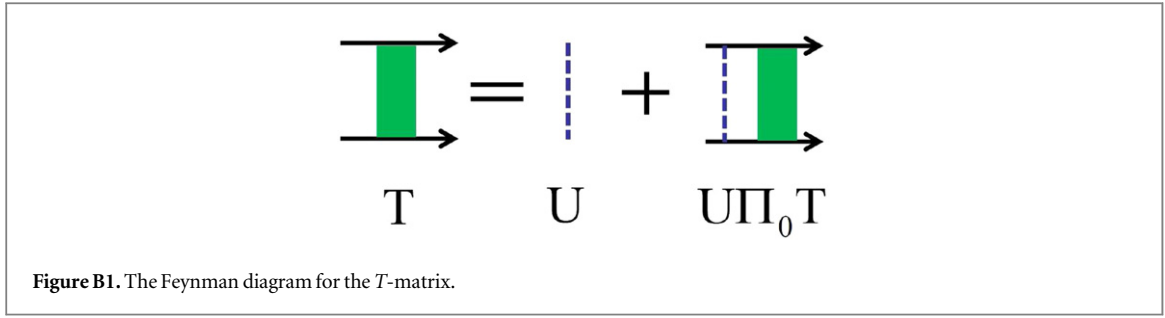
Figure B1. The Feynman diagram for the *T*-matrix.

Here, $E = k_1 + k_2$ is the total energy, the vacuum bubble $\Pi_0(E) = (E - \mathcal{H}_2)^{-1}$ is given in terms of $H_2 = \mathcal{H}_1 \otimes I_{2N} + I_{2N} \otimes \mathcal{H}_1$, and the interaction matrix **U** has the diagonal element $U_{ij}^{aa} = U_{ij}^{as} = U_{ij}^{sa} = U_0$ and $U_{ij}^{ss} = U_{ij}$ in the basis $\left\{ \left| a_i a_j \right\rangle, \left| a_i s_j \right\rangle, \left| s_i a_j \right\rangle, \left| s_i s_j \right\rangle \right\}$. The solution of equation (B.15) is $\mathbf{T}(E) = 1/(\mathbf{U}^{-1} - \Pi_0(E))$. The *S*-matrix can then be written as

$$S_{p_1+,p_2+;k_1+,k_2+}^{(2)} = T_{k_1} T_{k_2} \delta_{p_1 k_1} \delta_{p_2 k_2} - i \frac{\Gamma_{1D}^2}{8\pi} \delta_{p_1+p_2,k_1+k_2}$$

$$\times \sum_{ij;i'j'} \sum_{\sigma_1 \sigma_1';\sigma_2 \sigma_2'} \left[w^*(p_1, p_2) \right]_{ij}^{\sigma_1 \sigma_1'} [\mathbf{T}(E)]_{ij;i'j'}^{\sigma_1 \sigma_1';\sigma_2 \sigma_2'} \left[w(k_1, k_2) \right]_{i'j'}^{\sigma_2 \sigma_2'}$$

$$+ (p_1 \leftrightarrow p_2), \tag{B.16}$$

where

$$\left[w(k_1, k_2) \right]_{i'j'}^{\sigma \sigma'} = \sum_{j_1 j_2} e^{ik_{in}(z_{j_1} + z_{j_2})} \left[G_0(k_1) \right]_{i'j_1}^{\sigma a} \left[G_0(k_2) \right]_{j'j_2}^{\sigma' a}. \tag{B.17}$$

The Fourier transform of $S_{p_1+,p_2+;k_1+,k_2+}^{(2)}$ results in the wavefunction

$$\psi(x_c, x) = \int \frac{dp_1 dp_2}{2\pi} S_{p_1 p_2;k_1 k_2}^{(2)} e^{i(p_1 x_1 + p_2 x_2)}$$

$$= \frac{e^{iEx_c}}{2\pi} \left\{ 2 T_{\frac{E}{2}+k} T_{\frac{E}{2}-k} \cos(kx) - i \frac{\Gamma_{1D}^2}{4} \sum_{ij;i'j'} \sum_{\sigma_1 \sigma_1';\sigma_2 \sigma_2'} [F(x)]_{ij}^{\sigma_1 \sigma_1'} \right.$$

$$\left. \times [\mathbf{T}(E)]_{ij;i'j'}^{\sigma_1 \sigma_1';\sigma_2 \sigma_2'} \left[w\left(\frac{E}{2} + k, \frac{E}{2} - k \right) \right]_{i'j'}^{\sigma_2 \sigma_2'} \right\}, \tag{B.18}$$

of two transmitted photons, where the relative momentum $k = (k_1 - k_2)/2$, the center of mass coordinate $x_c = (x_1 + x_2)/2$, and the relative coordinate $x = x_1 - x_2$. The symmetric function

$$[F(x)]_{ij}^{\sigma \sigma'} = -i \sum_{i_1 i_2} \frac{e^{-ik_{in}(z_{i_1} + z_{i_2})}}{E - \varepsilon_l - \varepsilon_{l'}} \sum_{ll'} \chi_l(a_{i_1}) \chi_{l'}(a_{i_2})$$

$$\times \tilde{\chi}_l^*(\sigma_i) \tilde{\chi}_{l'}^*(\sigma_j') \left[e^{i\left(\frac{E}{2} - \varepsilon_{l'}\right)x} \theta(x) + e^{-i\left(\frac{E}{2} - \varepsilon_l\right)x} \theta(-x) \right]$$

$$+ (x \rightarrow -x) \tag{B.19}$$

is defined by the eigenstates $|\chi_l\rangle$ and $|\tilde{\chi}_l\rangle$ of $\mathcal{H}_1$ and $\mathcal{H}_1^\dagger$ with the corresponding eigenenergies ε_l and ε_l^*, with $\langle \sigma_i | \chi_l \rangle = \chi_l(\sigma_i)$ and $\langle \sigma_i | \tilde{\chi}_l \rangle = \tilde{\chi}_l(\sigma_i)$. Knowledge of the wave function (B.18) in the case where the two incident photons have the same momentum, $k_1 = k_2 = E/2$, enables one to calculate the second-order correlation function for the outgoing field, $g^{(2)}(x) = \left| \pi \psi(x_c, x)/T_{E/2}^2 \right|^2$.

We compare the result of $g^{(2)}(x)$ from the scattering theory and that from numerically solving the effective spin model (12) with the weak driving field in figure 4(c) in the main text, which shows that they agree with each other perfectly.

Appendix C. Generalized master equation

In this section, we extend our derivation of the atomic master equation, in order to calculate the response of the system to an arbitrary few-photon input state (as opposed to a classical or coherent state). The initial state is generally written as $|\psi_{in}\rangle = |\varphi_{in}\rangle \otimes |\chi_{in}\rangle$, where $|\chi_{in}\rangle$ is the initial state of the system, and

$$\left| \varphi_{\mathrm{in}} \right\rangle = \sum_{\left\{ n_{v,k} \right\}} \varphi_{\mathrm{in}} \left(\left\{ n_{v,k} \right\} \right) \prod_{k} \left| \left\{ n_{v,k} \right\} \right\rangle \tag{C.1}$$

describes an arbitrary state of incident photons in the Fock state basis by the wavefunction $\varphi_{\mathrm{in}}(\{n_k\})$. By the relation

$$\left| n \right\rangle = \lim_{J \to 0} \frac{1}{\sqrt{n!}} \frac{\partial^n}{\partial J^n} \left| J \right\rangle \tag{C.2}$$

between the Fock state $|n\rangle$ and the coherent state $|J\rangle = \sum_n J^n |n\rangle / \sqrt{n!}$, we rewrite $|\varphi_{\mathrm{in}}\rangle = \mathcal{F} |\{J_{v,k}\}\rangle$ by the operator

$$\mathcal{F} = \lim_{\left\{ J_{v,k} \right\} \to 0} \sum_{\left\{ n_k \right\}} \varphi_{\mathrm{in}} \left(\left\{ n_{v,k} \right\} \right) \prod_{k} \frac{1}{\sqrt{n_{v,k}!}} \frac{\partial^{n_{v,k}}}{\partial J_{v,k}^{n_{v,k}}} \tag{C.3}$$

acting on the coherent state $|\{J_k\}\rangle$.

The evolution of the reduced density matrix $\rho_s(t) = \mathrm{Tr}_b[\mathcal{U}(t)\rho(0)\mathcal{U}^\dagger(t)]$ is determined by

$$\mathcal{U}(t) = \mathcal{T} \exp\left[-\mathrm{i} \int_0^t \mathrm{d}s\, H(s) \right],$$

where $\rho(0) = |\psi_{\mathrm{in}}\rangle \langle \psi_{\mathrm{in}}|$ is the density matrix of the initial state, and $H(t)$ is the total Hamiltonian in the rotating frame with $b_{v,k} \to b_{v,k} \mathrm{e}^{-\mathrm{i}vkt}$. By the relation $|\varphi_{\mathrm{in}}\rangle = \mathcal{F} |\{J_{v,k}\}\rangle$, the reduced density matrix reads

$$\rho_s(t) = \mathcal{F}^* \mathcal{F} \, \mathrm{Tr}_b\left[\mathcal{U}(t) \left| \left\{ J_{v,k} \right\} \right\rangle \left\langle \left\{ J_{v,k} \right\} \right| \rho_s(0) \mathcal{U}^\dagger(t) \right], \tag{C.4}$$

where $\rho_s(0) = |\chi_{\mathrm{in}}\rangle \langle \chi_{\mathrm{in}}|$ is the initial density matrix of the system. The displacement transformation $V_{\mathrm{d}} |\{J_k\}\rangle = \mathrm{e}^{\frac{1}{2}\sum_{v,k}|J_{v,k}|^2} |0\rangle$ leads to

$$\rho_s(t) = \mathcal{F}^* \mathcal{F} \mathrm{e}^{\sum_{v,k} \left| J_{v,k} \right|^2} \rho_J(t), \tag{C.5}$$

and the generating density matrix

$$\rho_J(t) = \mathrm{Tr}_b\left[\mathcal{U}_{\mathrm{d}}(t) |0\rangle \langle 0| \, \rho_s(0) \mathcal{U}_{\mathrm{d}}^\dagger(t) \right], \tag{C.6}$$

where the unitary transformation

$$\mathcal{U}_{\mathrm{d}}(t) = \mathcal{T} \exp\left[-\mathrm{i} \int_0^t \mathrm{d}s\, H_{\mathrm{d}}(s) \right] \tag{C.7}$$

is given by $H_{\mathrm{d}}(s) = V_{\mathrm{d}} H(s) V_{\mathrm{d}}^\dagger$. The Hamitonian $H_{\mathrm{d}}(s) = H(s) + H_J(s)$ is obtained by replacing the operator $b_{v,k}$ by $b_{v,k} + J_{v,k}$ in the Hamiltonian $H(s)$, where $H_J(s)$ describes the system under the driving fields $J_{v,k}$. In the density matrix $\rho_J(t)$, the initial state becomes the vacuum state due to the displacement transformation, thus the evolution of $\rho_J(t)$ satisfies the master equation

$$\partial_t \rho_J(t) = \mathcal{L}\rho_J(t) - \mathrm{i}\left[H_J(t), \rho_J(t) \right], \tag{C.8}$$
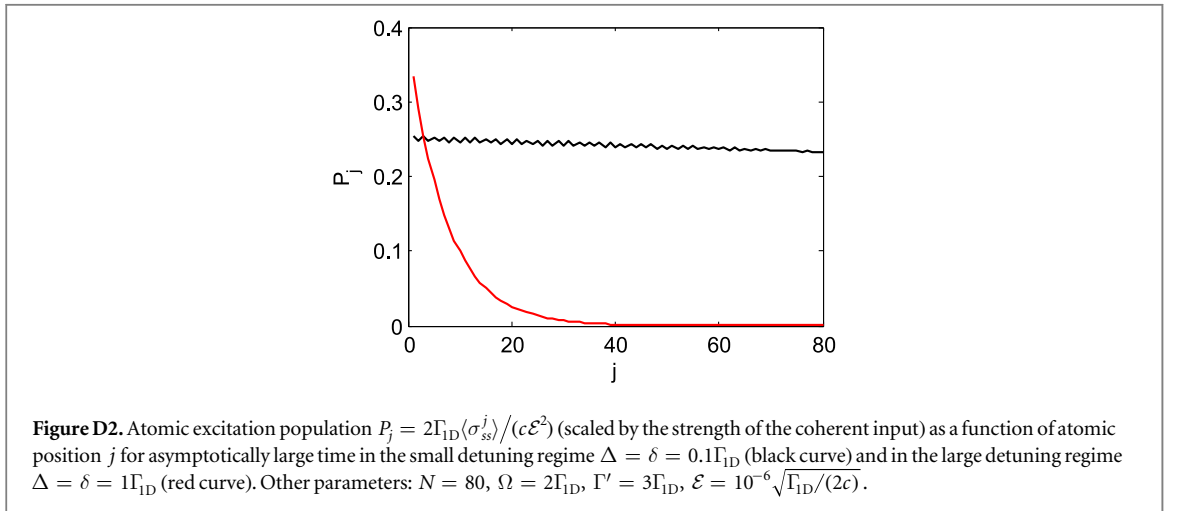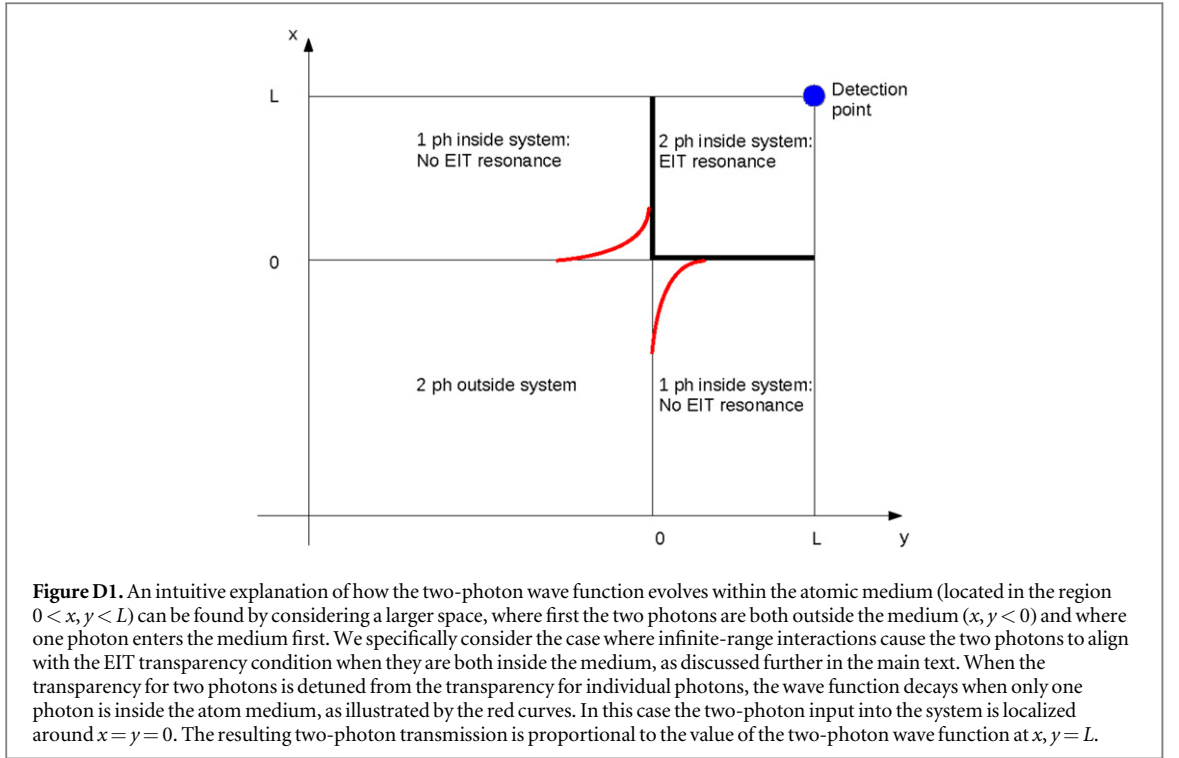
where $\mathcal{L}$ is the Lindblad super-operator of the system without H_J.

In conclusion, equation (C.5) establishes the relation bewteen the evolution of the reduced density matrix $\rho_s(t)$ for a few incident photons (which could be a non-classical state) and the evolution of the reduced density matrix $\rho_J(t)$ for the system with classical (coherent state) driving fields $J_{v,k}$. As a result, the few photon scattering problem can be understood as the perturbation expansion of the driving strength $J_{v,k}$.

Appendix D. Properties of two photon transmission T_2

In this section of the appendix we provide an intuitive explanation based on linear optics of the behavior of the two-photon transmission T_2 depicted in figures 4(a), (b). By indicating with x and y the coordinates of the first and second photons, we can divide the space into four regions according to their positions: both photons outside the atomic medium, one photon inside and one outside, and both photons inside the medium, see figure D1 . As we are studying an infinite-range interaction, within each region the evolution is effectively linear. The different dispersion relations in each region, however, lead to non-trivial boundary conditions at their edges. Relevant to our discussion is the value of the two-photon wave function at the boundaries $0 < x < L$ and $0 < y < L$. In particular, evolution in the region $0 < x, y < L$ with these boundary conditions dictates the two-photon transmission, which is proportional to the value of the two-photon wave function at $(x, y) = (L, L)$.
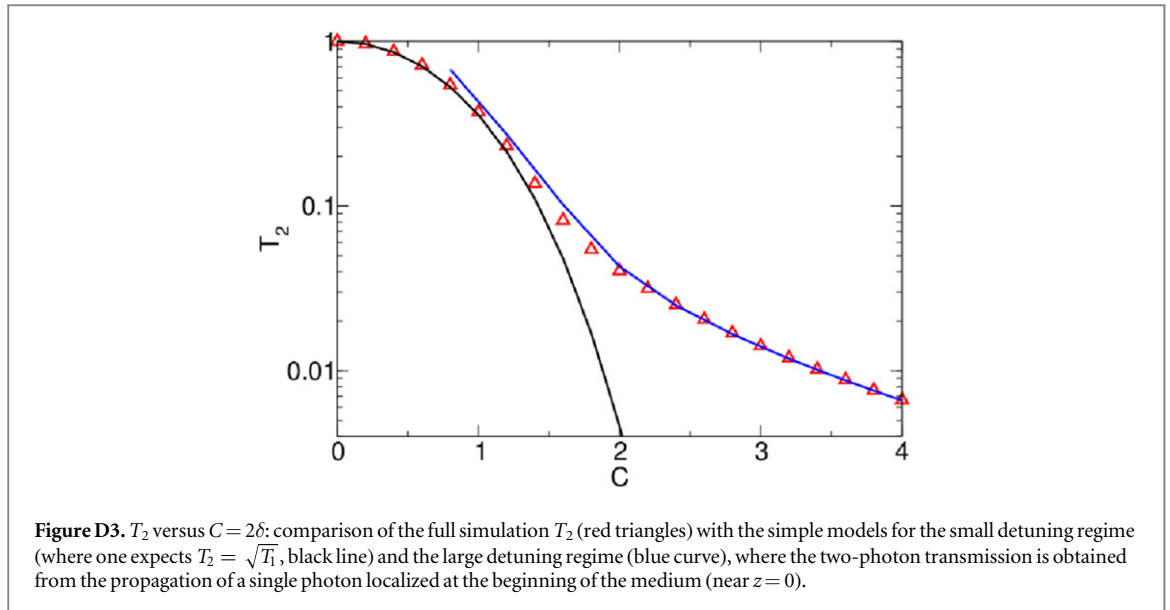
We study the case where the two photons have detunings $\Delta = C/2$. In this case, infinite-range interactions cause these two photons to satisfy the EIT transparency condition when both photons are inside the medium. Then, there are two qualitatively different regimes for the boundary values of the two-photon wave function,

Figure D1. An intuitive explanation of how the two-photon wave function evolves within the atomic medium (located in the region $0 < x, y < L$) can be found by considering a larger space, where first the two photons are both outside the medium ($x, y < 0$) and where one photon enters the medium first. We specifically consider the case where infinite-range interactions cause the two photons to align with the EIT transparency condition when they are both inside the medium, as discussed further in the main text. When the transparency for two photons is detuned from the transparency for individual photons, the wave function decays when only one photon is inside the atom medium, as illustrated by the red curves. In this case the two-photon input into the system is localized around $x = y = 0$. The resulting two-photon transmission is proportional to the value of the two-photon wave function at $x, y = L$.

Figure D2. Atomic excitation population $P_j = 2\Gamma_{1D}\langle\sigma_{ss}^j\rangle/(c\mathcal{E}^2)$ (scaled by the strength of the coherent input) as a function of atomic position j for asymptotically large time in the small detuning regime $\Delta = \delta = 0.1\Gamma_{1D}$ (black curve) and in the large detuning regime $\Delta = \delta = 1\Gamma_{1D}$ (red curve). Other parameters: $N = 80$, $\Omega = 2\Gamma_{1D}$, $\Gamma' = 3\Gamma_{1D}$, $\mathcal{E} = 10^{-6}\sqrt{\Gamma_{1D}/(2c)}$.

depending on the detuning from two-photon resonance δ (for simplicity we assume $\delta_L = 0$, so that $\Delta = \delta - \delta_L = \delta$): the small detuning regime, $\delta < \Delta_{EIT}$, in which a single photon can travel with high transmission through the medium and reach the detection point; and the large detuning regime, $\delta > \Delta_{EIT}$, in which a single photon is absorbed and cannot reach the detection point.

Small detuning regime. Within the first regime $\delta = C/2 < \Delta_{EIT}$, a single polariton still fits within the EIT transparency window and exhibits high transmission through the medium. In the case where the input field is constant, the atomic excitation population $\langle\sigma_{ss}^j\rangle$, which in the slow light regime corresponds to the distribution of polaritons, is largely uniform throughout the atomic medium, as illustrated by the black curve in figure D2. Now, we consider the two-excitation manifold. Because of the uniform distribution of single polaritons in the atomic medium and the random spacing of photons in the coherent input, a second photon entering the medium may be separated from the first by any distance between 0 and Nd. On average, the photons then travel a distance $Nd/2$ together in the medium, experiencing minimal loss, and $Nd/2$ experiencing loss as single photons would. Therefore we expect $T_2 = |\exp(-ik(\delta)Nd/2)|^2 = \sqrt{T_1}$. The predicted behavior is in good agreement with full simulations results as shown in figure D3 for small detuning.

Large detuning regime. In this regime a single photon is strongly absorbed. This is illustrated by the red curves in figure D2, where one observes a strong decay of the single-polariton probability and field intensity inside the

Figure D3. T_2 versus $C = 2\delta$: comparison of the full simulation T_2 (red triangles) with the simple models for the small detuning regime (where one expects $T_2 = \sqrt{T_1}$, black line) and the large detuning regime (blue curve), where the two-photon transmission is obtained from the propagation of a single photon localized at the beginning of the medium (near $z = 0$).

medium. Within the context of figure D1, this localized single excitation serves as the boundary condition on the segments $0 < x < L$ and $0 < y < L$. Furthermore, the evolution in the region $0 < x, y < L$ is effectively linear. Thus, the effect of this boundary condition at the detection point (a two-particle problem) can be mapped onto a simpler problem, wherein one studies how a single excitation, initialized in the shape of the localized photon given by the red curve, transmits through the medium. In this regime, we therefore can estimate that T_2 is twice the value of the maximum transmission associated with this single localized photon, whose evolution we calculate numerically.

The good agreement of our simplified estimates with full simulations is demonstrated in figure D3, in which T_2 as a function of $C = 2\delta$ is compared for the different cases.

References

[1] Chang D E, Vuletic V and Lukin M D 2014 *Nat. Photonics* **8** 685
[2] Kimble H J 2008 *Nature* **453** 1023
[3] Hartmann M J, Brandao F G S L and Plenio M B 2006 *Nat. Phys.* **2** 849
[4] Greentre A D, Tahan C, Cole J H and Hollenberg L C L 2006 *Nat. Phys.* **2** 856
[5] Angelakis D G, Santos M F and Bose S 2007 *Phys. Rev.* A **76** 031805(R)
[6] Chang D E *et al* 2008 *Nat. Phys.* **4** 884
[7] Otterbach J, Moos M, Muth D and Fleischhauer M 2013 *Phys. Rev. Lett.* **111** 113001
[8] Turchette Q A, Hood C J, Lange W, Mabuchi H and Kimble H J 1995 *Phys. Rev. Lett.* **75** 4710
[9] Birnbaum K M *et al* 2005 *Nature* **436** 87
[10] Vetsch E *et al* 2010 *Phys. Rev. Lett.* **104** 203603
[11] Goban A *et al* 2012 *Phys. Rev. Lett.* **109** 033603
[12] Bajcsy M *et al* 2009 *Phys. Rev. Lett.* **102** 203902
[13] Goban A *et al* 2014 *Nat. Commun.* **5** 3808
[14] Pritchard J D *et al* 2010 *Phys. Rev. Lett.* **105** 193603
    Pritchard J, Weatherill K and Adams C 2013 Nonlinear optics using cold Rydberg atoms *Annual Review of Cold Atoms and Molecules* ed K W Madison, Y Wang, A M Rey and K Bongs vol 1 (Singapore: World Scientific) pp 301–5
    Peyronel T *et al* 2012 *Nature* **488** 57
    Firstenberg O *et al* 2013 *Nature* **502** 71
    Baur S, Tiarks D, Rempe G and Durr S 2014 *Phys. Rev. Lett.* **112** 073901
[15] van Loo A F *et al* 2013 *Science* **342** 1494
[16] Hoi I-C *et al* 2013 *Phys. Rev. Lett.* **111** 053601
[17] Gardiner C W and Collett M J 1985 *Phys. Rev.* A **31** 3761
[18] Deutsch I H, Spreeuw R J C, Rolston S L and Phillips W D 1995 *Phys. Rev.* A **52** 1394
[19] Chang D E, Jiang L, Gorshkov A V and Kimble H J 2012 *New J. Phys.* **14** 063003
[20] Shi T and Sun C P 2009 *Phys. Rev.* B **79** 205111
[21] Fan S, Kocabas S E and Shen J-T 2010 *Phys. Rev.* A **82** 063821
[22] Zheng H, Gauthier D J and Baranger H U 2010 *Phys. Rev.* A **82** 063816
[23] Baragiola B Q, Cook R L, Brańczyk A M and Combes J 2012 *Phys. Rev.* A **86** 013811
[24] Pletyukhov M and Gritsev V 2015 *Phys. Rev.* A **91** 063841
[25] Zheng H, Gauthier D J and Baranger H U 2011 *Phys. Rev. Lett.* **107** 223601
[26] Roy D 2011 *Phys. Rev. Lett.* **106** 053601
[27] Shi T, Fan S and Sun C P 2011 *Phys. Rev.* A **84** 063803

[28] Laakso M and Pletyukhov M 2014 *Phys. Rev. Lett.* **113** 183601
[29] Redchenko E S and Yudson V I 2014 *Phys. Rev. A* **90** 063829
[30] Pletyukhov M and Gritsev V 2012 *New J. Phys.* **14** 095028
[31] Shi T, Chang D E and Cirac J I 2015 arXiv:1507.08699
[32] Lalumiere K *et al* 2013 *Phys. Rev. A* **88** 043806
[33] Meystre P and Sargent M III 1999 *Element of Quantum Optics* (New York: Springer)
[34] Xu S and Fan S 2015 *Phys. Rev. A* **91** 043845
[35] Fleischhauer M and Lukin M D 2002 *Phys. Rev. A* **65** 022314
 Fleischhauer M, Imamoglu A and Marangos J P 2005 *Rev. Mod. Phys.* **77** 633
[36] Chang D E, Safavi-Naeini A H, Hafezi M and Painter O 2011 *New J. Phys.* **13** 023003
[37] Gorshkov A V, Otterbach J, Fleischhauer M, Pohl T and Lukin M D 2011 *Phys. Rev. Lett.* **107** 133602
[38] Bienias P *et al* 2014 *Phys. Rev. A* **90** 053804
[39] Douglas J *et al* 2015 *Nat. Photonics* **9** 326
[40] Shahmoon E *et al* 2014 arXiv:1412.8331
[41] Mollow B R 1975 *Phys. Rev. A* **12** 1919
[42] Chang D E, Sorensen A S, Demler E A and Lukin M D 2007 *Nat. Phys.* **3** 807
[43] Sánchez-Burillo E, García-Ripoll J, Martín-Moreno L and Zueco D 2015 *Faraday Discuss.* **178** 335–56
[44] Pichler H, Ramos T, Daley A J and Zoller P 2015 *Phys. Rev. A* **91** 042116
[45] Guimond P-O, Roulet A, Le H N and Scarani V 2015 arXiv:1505.07908